Fisheries Science (2020) 86:1067–1078
https://doi.org/10.1007/s12562-020-01468-4

ORIGINAL ARTICLE

Environment

# Seasonal variations in phytoplankton productivity in a shallow cove in the eastern Seto Inland Sea, Japan

Hitomi Yamaguchi[1] · Nozomi Koga[1] · Kazuhiko Ichimi[2] · Kuninao Tada[1]

Received: 17 March 2020 / Accepted: 10 September 2020 / Published online: 1 October 2020


## Abstract

We examined phytoplankton productivity in Shido Bay, an active oyster farming area in the eastern Seto Inland Sea, Japan, by an in situ $^{13}C$ method from March 2016 to January 2017. The depth-integrated daily phytoplankton production ranged from 0.13 to 1.61 g C $m^{-2}$ $day^{-1}$, and the estimated annual production was 218 g C $m^{-2}$ $year^{-1}$. The daily production peaked in the rainy season and autumn, when phytoplankton blooms were observed, and production during the bloom events largely contributed to the annual production. There was a strong correlation between daily production and phytoplankton biomass (chlorophyll *a*) throughout the study period. In the study area, due to the shallow depth (6 m) and moderate light attenuation coefficient of the water column ($0.38 \pm 0.07$ $m^{-1}$), the mean light intensity in the water column was maintained at high levels ($36 \pm 5\%$ of incident photosynthetically active radiation) throughout the study period. In contrast, the dissolved inorganic nitrogen concentration of the water was persistently low (< 1.5 μM) from late winter to summer. As a consequence, an increase in nitrogen supply seemed to be the key factor causing the increases in daily production and directly triggering the phytoplankton blooms in the bay.

**Keywords** Phytoplankton · Biomass · Primary production · Dissolved inorganic nitrogen

## Introduction

Shido Bay, which covers an area of about 20 $km^2$ (Suenaga et al. 2002), is a cove on the Japanese coast of the eastern Seto Inland Sea (Fig. 1). This small cove is an important site for aquaculture (Srithongouthai and Tada 2017), especially suspended oyster culture (Inui 2013), because it provides shelter from strong winds and wave action. The annual yield of cultured oysters in Shido Bay represents a large proportion of the total annual oyster yield of Kagawa Prefecture (ca. 200 tons $year^{-1}$) (Inui 2013), which has the 11th highest oyster yield of all 47 Japanese prefectures (e-Stat 2019). Oyster farming is carried out without the addition of food as the suspended oysters feed directly on phytoplankton in the ambient seawater (Emmery et al. 2016). Therefore, the growth of oysters in Shido Bay is expected to be strongly influenced by local phytoplankton production, as was reported for other areas (Hirata and Akashige 2004; Cassis et al. 2011). Regarding the maintenance of sustainable fisheries in Shido Bay, it is thus important to quantify phytoplankton production (i.e., the integral phytoplankton productivity in the euphotic zone) and identify the factors that influence its variation. However, in contrast to some Japanese coastal areas with well-studied phytoplankton production [e.g., see Table 3 in Ara et al. (2011)], there is no published information on the productivity of Shido Bay.

Phytoplankton production is conceptually quantified as the growth rate of phytoplankton multiplied by its biomass [see Fig. 6 in Cloern et al. (2014)]. Phytoplankton growth

✉ Hitomi Yamaguchi
hitomiyjp@yahoo.co.jp

Nozomi Koga
koganozomidesu@gmail.com

Kazuhiko Ichimi
ichimi@ag.kagawa-u.ac.jp

Kuninao Tada
tada@ag.kagawa-u.ac.jp

[1] Faculty of Agriculture, Kagawa University, 2393 Ikenobe, Miki, Kita, Kagawa 761-0795, Japan

[2] Seto Inland Sea Regional Research Center, Kagawa University, 4511-15 Kamano, Aji, Takamatsu, Kagawa 761-0130, Japan

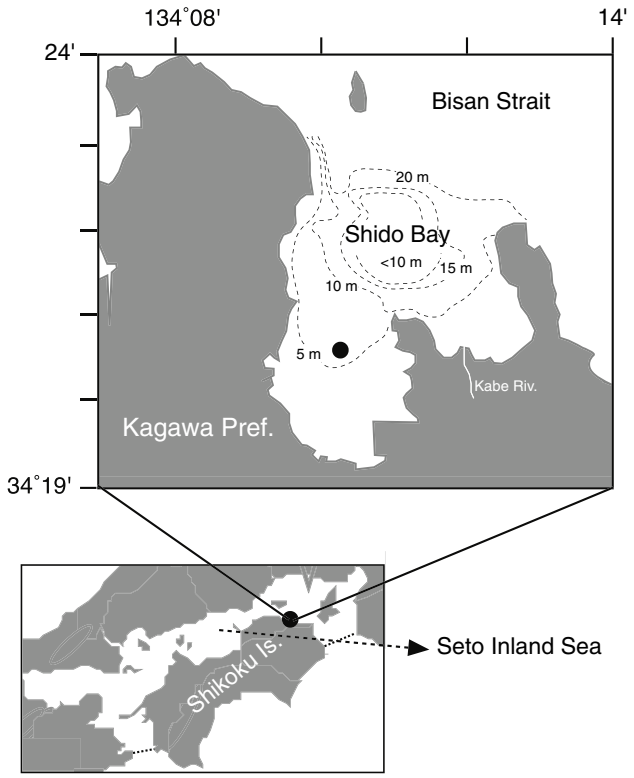


**Fig. 1** Geographic location of Shido Bay, eastern Seto Inland Sea, Japan. The *black circle* denotes the sampling site, station S. *Dotted lines* indicate isobaths. *Pref*. Prefecture, *Riv*. river, *Is*. island

is a physiological process that is generally affected by temperature, light availability, and/or nutrient concentrations (Örnólfsdóttir et al. 2004; Cloern et al. 2014). Changes in biomass result from an imbalance between biomass accumulation and loss, and are potentially affected by changes in growth rate and other factors. These factors include photoperiod, nutrient supply rate, feeding pressure from grazers, and physical transportation (Cloern et al. 2014). There is currently no information available on the growth-related parameters of phytoplankton in Shido Bay. Thus, it is interesting to explore which critical factors (i.e., temperature, light, and/or nutrients) regulate the growth rate of phytoplankton in this system, and how this growth contributes to variations in phytoplankton production. While there is some information available on the annual variation in the phytoplankton biomass in Shido Bay, it was based on water column chlorophyll *a* (Chl *a*) concentration (Tada and Morishita 1997; Kaeriyama et al. 2011; Yamaguchi et al. 2017). Kaeriyama et al. (2011) summarized monthly Chl *a* records obtained during the 2000s for Shido Bay. They indicated that the Chl-*a* level in this system usually does not peak in spring, which is the period when phytoplankton blooms usually occur in temperate areas, and instead reaches its highest values around late summer to early autumn. An autumn bloom of phytoplankton in Shido Bay was observed by Tada and Morishita (1997) in the mid-1990s and by Yamaguchi et al. (2017) in the early 2010s; hence, an autumn bloom seems to be a routine event in this system. The monthly data on Chl *a* presented by Yamaguchi et al. (2017) showed that high levels of Chl *a* were typically found on two successive sampling dates from late August to October. Therefore, to understand the dynamics of phytoplankton production in Shido Bay, it is considered informative to determine what triggers the autumn bloom, and to what extent the variation in phytoplankton production relies on such bloom events.

In this study, we investigated seasonal variations in phytoplankton biomass, phytoplankton productivity, and Chl *a* specific productivity, i.e., assimilation number, an index of the phytoplankton growth rate (e.g., Eppley 1972; Shiomoto 2011), at a site in Shido Bay for approximately 1 year. The objectives of the study were (1) to evaluate the absolute annual phytoplankton production in Shido Bay by comparing it with that of other subareas of the Seto Inland Sea, (2) to clarify how the magnitude of phytoplankton production is maintained in the bay, and (3) to identify the main factors that regulate the seasonal variation in phytoplankton production in the bay.

## Materials and methods

### Sampling site

Shido Bay has a mean depth of 8 m (Suenaga et al. 2002); the water in the bay is mostly shallow with a depth of less than 10 m (Fig. 1). The bay opens into the Bisan Strait, where strong tidal currents occur, and the water exchange between the bay and the strait is a key determinant of the water quality in the bay (Miyagawa and Fujiwara 2011). The main freshwater input into the bay is from the Kabe River (Srithougthai et al. 2003). The annual freshwater discharge from the Kabe River into the bay in 2002 was estimated to be about $2 \times 10^7$ m$^3$ year$^{-1}$ (Dr. M. Ishizuka, personal communication). Due to the shallowness and moderate light attenuation of the seawater in the bay, the entire water column is often considered an euphotic layer (Yamaguchi et al. 2017). In the present study, all the sampling was conducted at a site [station (Stn) S] where phytoplankton biomass and related parameters have been investigated in previous studies (Tada and Morishita 1997; Kaeriyama et al. 2011; Yamaguchi et al. 2017). This site has a mean depth of 6 m and is located in the inner part of western Shido Bay, which is the main area used for oyster farming.

## Field sampling and data collection

We conducted field sampling on 16 occasions at Stn S from March 2016 to February 2017 aboard the research vessel (R/V) Calanus III. We generated vertical profiles of the water column temperature, salinity, and downwelling photosynthetically active radiation (PAR) during each cruise using a conductivity-temperature-depth (CTD) sensor equipped with an underwater quantum sensor (AAQ-1183; JFE Advantech, Japan). The CTD sensor was deployed on the sunny side of the vessel to avoid shading effects. The vertical profile of the downwelling PAR from 0.5 m below the surface to 0.5 m above the bottom was used to calculate the attenuation coefficient of PAR in the water column ($K_d$). The calculation of $K_d$ was based on the Lambert–Beer law, as described in Foden et al. (2008). On 14 of the 16 sampling dates, when phytoplankton productivity was examined (see below), the mean PAR intensity in the water column ($I_m$) was also calculated based on the following equation (Riley 1957; Ho et al. 2010):

$$I_m = I_0\{1 - \exp(-K_d z)\}(K_d z)^{-1} \quad (1)$$

where $I_0$ (mol $m^{-2}$ $day^{-1}$) is the intensity of PAR just below the sea surface, and $z$ denotes the mean water depth at Stn S (6 m). We measured the PAR in the surface air (incident PAR) at the Aji Marine Station, Kagawa University, located about 5 km from Stn S, using a LI-190 Quantum Sensor (LI-COR, USA). The loss rate of solar energy at the sea surface varies owing to the conditions at the sea surface as well as the angle of the sun, but a mean value of 15% is often used as an approximation for field studies of phytoplankton (Parsons et al. 1984). Here, taking into consideration the sheltered location of Shido Bay, an $I_0$ was calculated from the incident PAR with an assumed mean of 10% for the total surface losses.

After measurements were taken using the CTD sensor, we collected seawater from four layers (0-, 2-, 4-, and 5-m depth) using a plastic bucket and a Van Dorn water sampler. These samples were used to analyze the water nutrient and Chl *a* concentrations, and to measure phytoplankton productivity.

In addition to our own sampling, we obtained daily records of global solar radiation and precipitation for the period from March 2016 to February 2017, which were measured about 10 km from Stn S by the Japan Meteorological Agency (JMA) (https://www.jma.go.jp/jma/indexe.html). Daily global solar radiation data were used to estimate the daily incident PAR based on the empirical relationship reported by Koga (1990). Daily precipitation was summed to calculate the total precipitation of each half-month period.

## Nutrient and Chl *a* analysis

For the nutrient analysis, seawater samples were filtered through a 0.45-μm DISMIC cellulose acetate filter (Advantec, Japan). The filtrates were transferred to polypropylene tubes and stored at − 20 °C until analyses were performed. The dissolved silicic acid (DSi), dissolved inorganic phosphorus (DIP), $NO_2 + NO_3$-N, and $NH_4$-N concentrations in the filtrates were determined simultaneously by colorimetry using an Auto Analyzer III (BL Tec, Japan), as described in the manuals supplied by the instrument supplier. Hereinafter, we refer to the sum of the $NO_2 + NO_3$-N and $NH_4$-N as dissolved inorganic nitrogen (DIN).

For the Chl *a* analysis, a known volume of seawater was filtered through a Whatman GF/F filter. The retained phytoplankton were soaked in 90% acetone, stored in cool and dark conditions, and then sonicated. The solvent was subsequently filtered through a 0.45-μm polytetrafluoroethylene Ekicrodisk (Nihon Pall, Japan) to remove suspended solids. The concentration of the extracted Chl *a* was determined by the fluorometric acidification method (Holm-Hansen et al. 1965) using a 10-AU fluorometer (Turner Designs, USA). The fluorometer was calibrated for pure Chl *a* based on the molar absorption coefficient reported by Jeffrey and Humphrey (1975).

We calculated the mean concentration of each nutrient and the depth-integrated Chl *a* (i.e., phytoplankton biomass) in the water column by assuming that the water depth was always 6 m, and that the concentration of each respective parameter at 6-m depth was equal to that at 5-m depth.

## Measurement of phytoplankton productivity

On 14 of the 16 sampling dates, from March 2016 to January 2017, we measured phytoplankton productivity using the in situ $^{13}C$ method. On each sampling date, the seawater taken from each depth (i.e., 0, 2, 4, and 5 m) was subsampled to determine the total inorganic carbon concentration by the method of Strickland and Parsons (1972). The rest of the seawater sampled from each depth was passed through a 220-μm mesh to remove large zooplankton. Then, 500 ml of the mesh-filtered seawater was subsequently transferred into acid-washed light and dark Nalgene polycarbonate bottles, and each bottle was inoculated with 100 μmol $NaH^{13}CO_3$.

In situ incubation was initiated around noon, and performed for 2–3 h (Rysgaard et al. 1999; Timothy and Soon 2001; Tada et al. 2001). During incubation, the bottles were suspended at each sampled depth by a rope from the ship, which was positioned away from the vessel. The incubated seawater and zero-time blank samples were each filtered immediately onboard the ship with a precombusted Whatman GF/F filter. The filters were treated with acid to remove carbonates and then desiccated. The

particulate organic carbon concentration and the atomic percentage (atom%) of $^{12}C$ and $^{13}C$ on each filter were then analyzed by SI Science, Japan, using a mass spectrometer (Flash2000-DELTA$^{plus}$ Advantage ConFlo III System; Thermo Fisher Scientific, USA). Phytoplankton productivity during the incubation period at each depth (μg C $l^{-1}$ $h^{-1}$) was calculated based on the method of Hama et al. (1983). Then, the dark uptake was subtracted from the light uptake. We also calculated Chl *a* specific productivity (mg C $mg^{-1}$ Chl *a* $h^{-1}$) by dividing the hourly productivity by the Chl *a* concentration. To calculate phytoplankton production during the incubation period (mg C $m^{-2}$ $h^{-1}$), the trapezoidal depth integration of phytoplankton productivity was applied. We assumed that the water depth was always 6 m and that the productivity at 6-m depth was equal to that at 5-m depth. Daily phytoplankton production (g C $m^{-2}$ $day^{-1}$) was obtained by multiplying the phytoplankton production measured during the incubation period by a PAR factor, i.e., the ratio of the PAR available during a short-term incubation to that available over a 24-h period (e.g., Rysgaard et al. 1999; Tada et al. 2001; Timothy and Soon 2001; Adachi and Nakayama 2009; Grundle et al. 2009; Ho et al. 2010). This calculation assumes that carbon assimilation by the phytoplankton assemblages at each time point within a day is proportional to the PAR.

We calculated the phytoplankton production for each month (g C $m^{-2}$ $month^{-1}$) using the data from two successive sampling dates on the basis of the trapezoidal integration. Note that the production in March 2016 and January 2017 (the first and final month) was based on a single day measurement. Furthermore, we estimated the production in February 2017 by applying a linear interpolation using the data for January 2017 and March 2016. We finally obtained the annual phytoplankton production (g C $m^{-2}$ $year^{-1}$) by summing the production of 12 months from March 2016 to February 2017.

### Statistics

To assess the relationship between two variables, a simple linear regression analysis was performed. We conducted multiple linear regression analysis to evaluate which factor(s) was related to the variability of the mean Chl *a* specific productivity in the water column, based on the stepwise forward selection method using multivariate analysis statistical software for Macintosh (Esumi, Japan). Then, $F_{in} = 2.0$ and $F_{out} = 2.0$ were used as the criteria. Because phytoplankton growth is directly regulated by light intensity, temperature, and/or nutrient concentrations (e.g., Cloern et al. 2014), we considered $I_m$, mean temperature, and mean nutrients in the water column as explanatory variables.

## Results

### Temperature and salinity

The mean water temperature in the water column (Fig. 2a) increased from March (11.9 °C) to August (28.5 °C), and thereafter decreased over time until February (8.4 °C). Thermal stratification, defined herein as occurring when there were vertical temperature differences larger than 0.5 °C, was observed from March to August. This stratification disappeared in September, when sea surface cooling was initiated. Salinity was almost always homogeneous in the vertical plane, and the mean value in the water column ranged between 30.5 and 32.0 (Fig. 2b). Minimum salinity values were recorded from June to early July and in September, during periods of high precipitation (Fig. 2c).

### Light-related parameters

The measured attenuation coefficient of PAR in the water column ($K_d$) ranged between 0.26 and 0.55 $m^{-1}$, with a mean of 0.38 $m^{-1}$, and the entire water column was always penetrable to > 1% of the surface PAR (data not shown). As a result, the mean PAR available in the water column ranged between 26 and 45% of the incident PAR, with a mean of 36% (Fig. 2d). Temporal variation in the daily $I_m$ (Fig. 2d), which is a function of $K_d$ (i.e., the PAR attenuation rate) and the intensity of incident PAR, was affected strongly by the incident PAR (Fig. 2e), but not by the $K_d$. The daily $I_m$ varied seasonally, with maximum values in May and August (24.8 and 23.9 mol $m^{-2}$ $day^{-1}$, respectively) and minimum values in late October (6.1 mol $m^{-2}$ $day^{-1}$).

### Nutrients

The mean DSi concentration in the water column (Fig. 3a) increased from March onward, peaked in June–July (21.9–24.8 μM) and in late October (30.1 μM), and thereafter decreased until February (4.1 μM). The mean DIN concentration in the water column (Fig. 3b) remained at low levels (0.6–1.2 μM) until August, and then increased thereafter, and the highest level was recorded in December. Seasonal variations in the mean DIP concentration in the water column (Fig. 3c) were more similar to those of DIN than those of DSi, but unlike DIN, DIP levels gradually increased from March to August. Differences in nutrient concentrations in the vertical plane were usually small (Fig. 3d–f), with a few exceptions. The molar ratio of DIN:DIP at each sampling date and depth was consistently

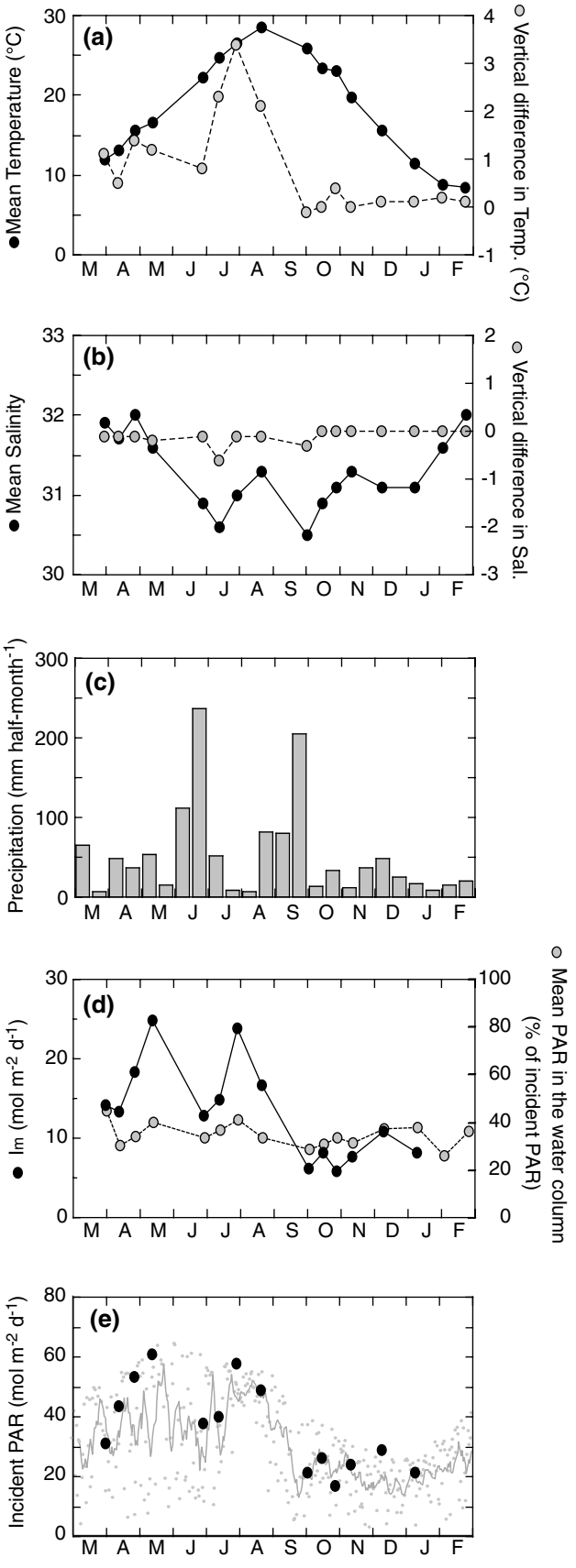


**Fig. 2** Temporal variations in **a** mean temperature (*Temp.*) at 0- to 5-m depth and vertical differences in temperature in the water column, **b** mean salinity (*Sal.*) at 0- to 5-m depth and vertical differences in salinity in the water column, **c** precipitation during half-monthly periods, **d** mean photosynthetically active radiation (*PAR*) intensity in the water column ($I_m$) and its % relative to the incident PAR, and **e** intensity of incident PAR. **e** *Gray dots* Incident PAR estimated from global solar radiation, *gray line* 7-day (*d*) moving average of the estimated incident PAR, *black circles* incident PAR measured during sampling (see text)

less than 16, whereas the DSi:DIN and DSi:DIP ratios were almost always higher than 1 and 16, respectively (Fig. 4).

## Phytoplankton biomass and productivity

Seasonal variations in the depth-integrated Chl *a* (i.e., phytoplankton biomass) in the water column (Fig. 5a) showed a bimodal pattern, with peaks in June (27 mg $m^{-2}$) and September–October (26–53 mg $m^{-2}$). In these periods, the Chl *a* concentration was elevated throughout the water column (Fig. 5d), and the highest value measured in the water column at each sampling date was over 5 µg $l^{-1}$. Except for the two peak periods, the Chl *a* concentration was typically around 1–2 µg $l^{-1}$ in the entire water column, and the biomass was consequently less than 15 mg $m^{-2}$. The linear regression analysis indicated that the phytoplankton biomass was moderately correlated with the water column mean DSi concentration ($r = 0.54$, $n = 16$, $p < 0.05$), whereas there were no significant ($p > 0.05$) relationships between the biomass and water column mean DIN or DIP concentrations.

Phytoplankton productivity ranged between 18 and 488 µg C $l^{-1}$ $day^{-1}$, and varied vertically as well as temporally (Fig. 5f). The maximum rate at each sampling date was usually recorded in the surface layer (0–2 m) and typically decreased with depth, with the minimum rate at each date often observed at the bottom (5 m). The maximum rate was not more than twice the minimum rate for most (ten of 14) sampling dates, but was six times higher than the minimum in September.

Chl *a* specific productivity was higher than 2 µg C $µg^{-1}$ Chl *a* $h^{-1}$ in the entire water column for 11 of the 14 sampling dates (Fig. 5e). In July–August, the Chl *a* specific productivity often exceeded 10 µg C $µg^{-1}$ Chl *a* $h^{-1}$ at the surface (0–2 m), and was higher than 5 µg C $µg^{-1}$ Chl *a* $h^{-1}$ even in the deeper 4- to 5-m layer. The mean productivity in the water column (Fig. 5b) consequently ranged from 2.1 to 9.1 µg C $µg^{-1}$ Chl *a* $h^{-1}$, with an overall mean of 4.8 µg C $µg^{-1}$ Chl *a* $h^{-1}$. The results of the stepwise multiple regression analysis using temperature, $I_m$, and different nutrients as explanatory variables indicated that the mean Chl *a* specific productivity in the water column was significantly and

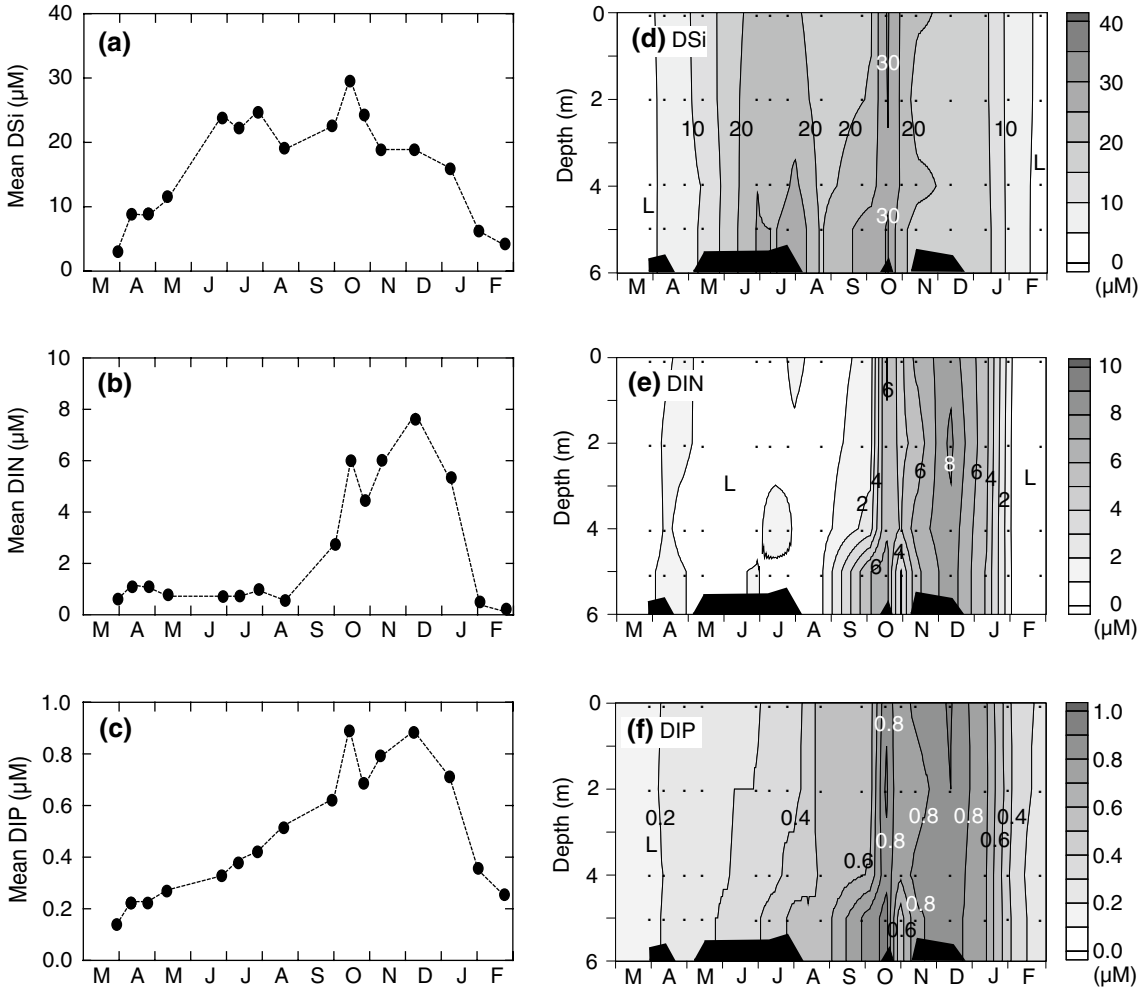


**Fig. 3** Temporal variations in **a** mean dissolved silicic acid (*DSi*) concentration in the water column, **b** mean dissolved inorganic nitrogen (*DIN*) concentration in the water column, **c** mean dissolved inorganic phosphorus (*DIP*) concentration in the water column, **d** vertical distribution of DSi, **e** vertical distribution of DIN, and **f** vertical distribution of DIP. Means were calculated by assuming that the water depth was 6 m (see Materials and methods)

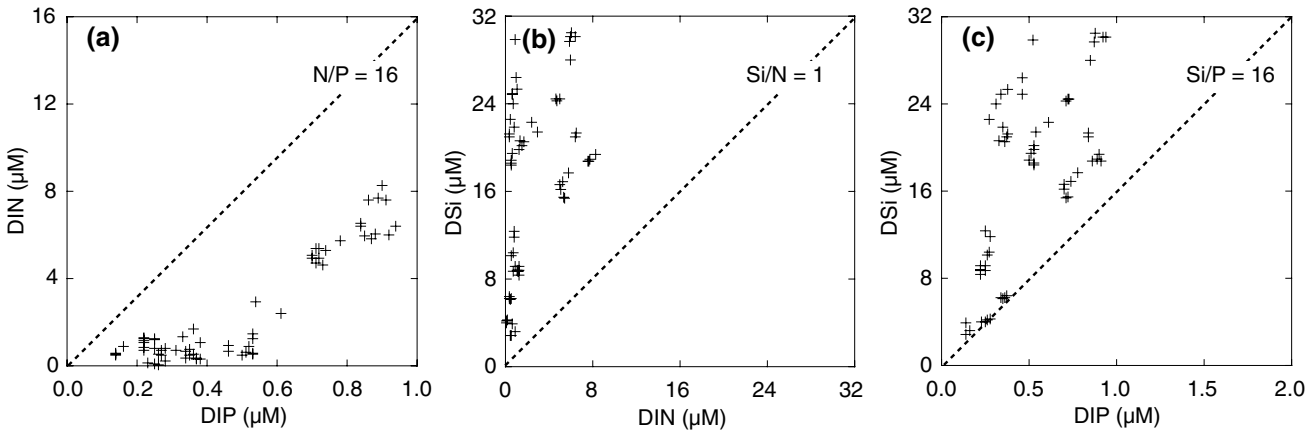


**Fig. 4** Scatterplots of **a** DIP versus DIN, **b** DIN versus DSi, and **c** DIP versus DSi. *Dotted lines* indicate DIN:DIP (*N*/*P*) = 16 (**a**), DSi:DIN (*Si*/*N*) = 1 (**b**), and DSi:DIP (*Si*/*P*) = 16 (**c**). For abbreviations, see Fig. 3

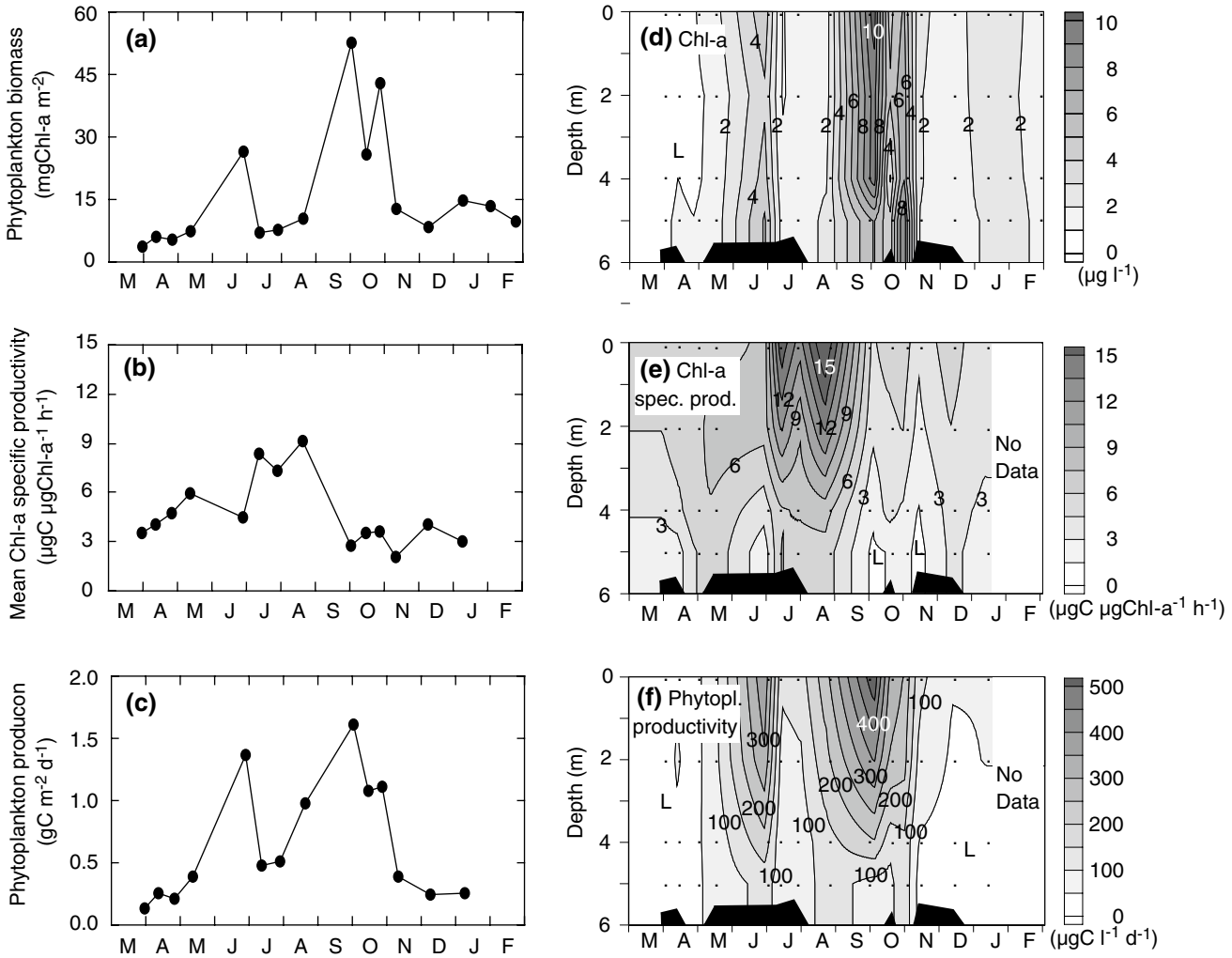


**Fig. 5** Temporal variations in **a** depth-integrated phytoplankton biomass, **b** mean chlorophyll *a* (Chl *a*) specific productivity in the water column, **c** daily phytoplankton production, **d** vertical distribution of Chl *a*, **e** vertical distribution of Chl *a* specific productivity, and **f** vertical distribution of daily phytoplankton productivity. Depth-integrated values and means were calculated by assuming that the water depth was 6 m (see Materials and methods)

positively related to $I_m$ and mean temperature; the equation is expressed as follows:

$$\text{Mean Chl } a \text{ specific product.} = 0.18 \times \text{Temp.} + 0.24 \times I_m - 1.95 \left(R^2 = 0.70,\ n = 14, p < 0.01\right) \quad (2)$$

Both of the two explanatory variables were significant ($p < 0.05$), and the standardized partial regression coefficients of temperature and $I_m$ were 0.49 and 0.67, respectively.

The depth-integrated daily phytoplankton production (Fig. 5c) ranged from 0.13 to 1.61 g C m$^{-2}$ day$^{-1}$, with peaks in June (1.37 g C m$^{-2}$ day$^{-1}$) and September–October (1.08–1.61 g C m$^{-2}$ day$^{-1}$). The seasonal variation in this variable was strongly and positively correlated with phytoplankton biomass (Fig. 6). On the contrary, no significant relationship was observed between phytoplankton production and the water column mean Chl *a* specific productivity ($r = -0.03$, $n = 14$, $p > 0.05$). The annual phytoplankton production was estimated to be 218 g C m$^{-2}$ year$^{-1}$.

## Discussion

### Phytoplankton production methodology

An incubation of 12- to 24-h duration is the standard when estimating daily phytoplankton production by carbon tracer and oxygen methods. However, daily phytoplankton production estimated by long-term incubation is considered problematic as this method is time-consuming and increases the risk of artifacts as a result of the longer confinement of samples in bottles (Lohrenz 1993; Cloern 2014). Thus,

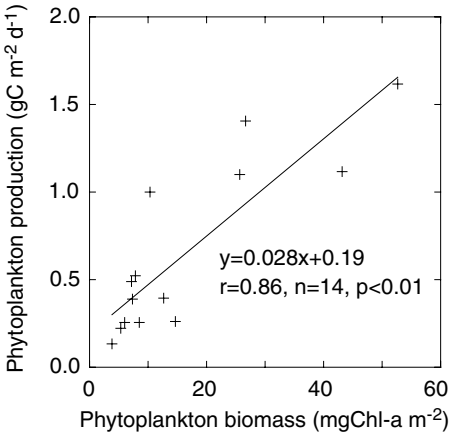


**Fig. 6** Relationship between phytoplankton biomass and daily phytoplankton production during the study period. The *plotted line* represents the regression line fit to the data based on the least-squares method

similarly to Tada et al. (2001), we chose to use a short-term (2–3 h) incubation in the present study to minimize bottle effects and save time.

It is generally assumed that the phytoplankton production estimates obtained by 12- to 24-h incubations based on carbon tracer methods represent net production (e.g., Hashimoto and Saino 2004). On the other hand, measurements obtained during incubations of only a few hours seem to represent gross production (e.g., Dring and Jewson 1982), although this is still debated. As discussed in the section below, most studies, including the present one, that use carbon tracer methods to assess phytoplankton production in subareas of the Seto Inland Sea employ 2- to 6-h incubation periods. This suggests that the reported rates for the Seto Inland Sea discussed below represent either gross production rather than net production or rates somewhere between these two, depending on the incubation time.

## Annual phytoplankton production

We examined phytoplankton productivity on 14 occasions during approximately 1 year in Shido Bay. Phytoplankton production in different subareas of the Seto Inland Sea has been previously reported (e.g., Endo 1970; Yamaguchi and Anraku 1984; Joh 1986; Uye et al. 1987; Yamaguchi et al. 1995; Yamaguchi and Imai 1996; Tada et al. 1998; Genkai-Kato et al. 2008). However, only a few studies reported depth-integrated annual phytoplankton production that was based on measurements taken at least monthly (Endo 1964; Tada et al. 2001; Yamashita et al. 2011; Yamaguchi et al. 2015; Ohara et al. 2020). When compared to the estimates obtained in these studies, which employed high-frequency sampling, the annual phytoplankton production in Shido Bay is similar to that in Shitaba Bay, located in the Uwa Sea in the Bungo Channel [168–226 g C $m^{-2}$ $year^{-1}$ (Yamashita et al. 2011)] and in Dokai Bay in the Hibiki-nada Sea [180 g C $m^{-2}$ $year^{-1}$ (Tada et al. 2001)]. On the other hand, the calculated rate is somewhat higher than that reported for the adjacent area, the Bisan Strait [163 g C $m^{-2}$ $year^{-1}$ (Yamaguchi et al. 2015)].

Tada et al. (1998) measured phytoplankton production four times a year for the whole Seto Inland Sea and estimated the annual rate to be 218 g C $m^{-2}$ $year^{-1}$. This is the latest published figure on phytoplankton production for the entire Seto Inland Sea. If we assume that this rate is representative of the area and has not changed markedly between that study and the present (Nakai et al. 2018), then the annual production in Shido Bay is comparable to the overall mean production of the Seto Inland Sea. The mean depth of the euphotic layer is 22 m for the entire Seto Inland Sea (Tada et al. 1998), whereas in Shido Bay it is 6 m (i.e., the water depth). This indicates that the annual phytoplankton production in Shido Bay is relatively high, when we take into account its shallow euphotic layer. In the entire Seto Inland Sea, the phytoplankton biomass and mean Chl *a* specific productivity in the euphotic layer were reported to be 45 mg Chl *a* $m^{-2}$ and 2.3 μg C $μg^{-1}$ Chl *a* $h^{-1}$ on average, respectively (Tada et al. 1998). The mean biomass ($17 \pm 15$ mg Chl *a* $m^{-2}$; Fig. 5a) in Shido Bay is lower, but the Chl *a* specific productivity ($4.8 \pm 2.1$ μg C $μg^{-1}$ Chl *a* $h^{-1}$; Fig. 5b) is higher than that for the entire Seto Inland Sea, based on data reported by Tada et al. (1998). Therefore, the relatively high annual production of the shallow Shido Bay seems to be at least partly related to its relatively high rate of Chl *a* specific productivity.

Yamaguchi et al. (1995) examined Chl *a* specific productivity during a 1.5-year period in Hiroshima Bay at 2-m depth, and reported that the mean productivity (based on the net photosynthetic rate) was 6.1 μg C $μg^{-1}$ Chl *a* $h^{-1}$. In Shitaba Bay, the Chl *a* specific productivity at < 6-m depth was rarely < 2 μg C $μg^{-1}$ Chl *a* $h^{-1}$ throughout the year, and was frequently > 10 μg C $μg^{-1}$ Chl *a* $h^{-1}$ during the summer (Fig. 4c in Yamashita et al. 2011). The results from these previous reports suggest that the observed Chl *a* specific productivity in water shallower than 6-m depth in Shido Bay (Fig. 5b) is typical for the upper euphotic zone in the Seto Inland Sea. In Shido Bay, the mean PAR levels in the water column remained high at $36 \pm 5$% of the incident PAR throughout the year (Fig. 2d). Furthermore, the observed $I_m$ ($13.3 \pm 6.1$ mol $m^{-2}$ $day^{-1}$) was always higher than the irradiance of the half-saturation constant for coastal phytoplankton growth (2.4 mol $m^{-2}$ $day^{-1}$) suggested by Cloern (1999), as well as the compensation irradiance for natural phytoplankton assemblages (Marra 2004). Therefore, it is reasonable to conclude that the high average PAR seen in Shido Bay is able to support higher mean values of Chl *a*

specific productivity in the euphotic layer compared to the overall average productivity in the Seto Inland Sea.

## Seasonal variation in phytoplankton production

Variations in phytoplankton production are caused by changes in both the biomass and physiological state of phytoplankton, but the relative importance of these factors depends on situation. Marañón et al. (2003) reported that independent variations in phytoplankton production and biomass are often observed in oligotrophic open-ocean areas. Hence, they emphasized the necessity for an accurate description of physiological variability when estimating productivity. On the other hand, significant coupling between production and biomass has been reported for several areas, such as in coastal upwelling areas in Chile (Montecino and Quiroz 2000; Daneri et al. 2000), Saanich Inlet in Canada (Grundle et al. 2009), and Sagami Bay in Japan (Ara et al. 2019).

In Shido Bay, there was a high correlation between the daily production and phytoplankton biomass throughout the study period (Fig. 6), whereas phytoplankton production did not exhibit a significant relationship with Chl *a* specific productivity. Even when the mean water column Chl *a* specific productivity reached its second and third highest levels in the year, both phytoplankton production and biomass remained low (Fig. 5a–c). These results suggest that variations in phytoplankton production in Shido Bay depend on its biomass, rather than on its physiological state (i.e., growth rate).

In terms of the temporal variation in phytoplankton production measured in Shido Bay, there were two considerable peaks of phytoplankton biomass (i.e., periods of phytoplankton blooms). One bloom occurred in June and the other in the autumn, the latter persisting for approximately 1 month (September–October) (Fig. 5a,c). When the measurements of phytoplankton production on the bloom dates were not taken into account and the annual production was recalculated from data for the other dates by trapezoidal integration, the recalculated production was 31% less than the actual annual rate (149 vs. 218 g C $m^{-2}$ $year^{-1}$). This estimate suggests that phytoplankton production during the bloom events contributed largely to the annual phytoplankton production.

The occurrence of the two bloom events in this system may be closely related to the nitrogen dynamics therein. Nitrogen was considered the most deficient nutrient from the stoichiometric nutrient balance, irrespective of sampling date and depth. This was based on the results shown in Fig. 4, with the assumption that the representative atomic ratio of DIN:DIP:DSi consumed by phytoplankton communities (planktonic diatoms) is 16:1:16 (Fisher et al. 1992; Justić et al. 1995).

June, when the first bloom occurred, falls within the rainy season in Japan. The monthly precipitation in June 2016 (349 mm $month^{-1}$) was three times higher than the average monthly precipitation over the 12 months of the study period (105 mm $month^{-1}$), and the highest recorded precipitation value of the study period (Fig. 2c). Tada (1998) examined the DIN concentration of rainwater in Kagawa Prefecture over a 3-year period and reported an annual mean concentration of 58 µM. Thus, the nitrogen input from rainfall was expected to be highest in June, and an estimated additional supply of 14 mmol N $m^{-2}$ $month^{-1}$ (i.e., 58 µM N × 349–105 mm) would have been provided then relative to that supplied in a normal month. High precipitation also tends to increase the freshwater and nitrogen inputs from rivers. As Japanese rivers generally have dams and barrages, an abrupt increase of freshwater and nitrogen discharge is reported for some rivers soon after a high precipitation event (e.g., Tanaka et al. 2009). The Kabe River, the main river flowing into Shido Bay, has a dam in its upper stream and an estuary barrage. There is little information on river water discharge around Shido Bay, including from the Kabe River, but it is possible that the nitrogen input from rivers into Shido Bay increased in June. In addition, Kaeriyama et al. (2011) suggested that salinity in Shido Bay might be affected by freshwater discharges that occur 1 month earlier from large rivers along the northern coast of Harima-Nada, tens of kilometers from Shido Bay. Although nutrients are non-conservative substances and may be consumed during transportation, riverine nutrient supply from the outer bay might not be negligible. Despite the increased nitrogen supply in June, the DIN concentration did not increase then (Fig. 3b). However, for DSi, the most abundant and sufficient nutrient of the three nutrients measured based on the stoichiometric balance (Fig. 4), a considerable peak was observed in June (Fig. 3a). This suggests that any additional nitrogen, supplied either directly or indirectly derived from precipitation, was completely consumed in this period, which may explain why a low DIN concentration accompanied by high phytoplankton biomass was recorded in June. The half-saturation constants for phytoplankton growth with respect to nitrogen and for the nitrogen uptake of phytoplankton are highly variable, yet 1.5 µM (Cloern 1999) and similar levels, e.g., 1–2 µM (Fisher et al. 1992; Justić et al. 1995), are traditionally assumed in field studies. If we employ such "threshold" values, the DIN level is considered to be low in June with respect to the absolute nitrogen concentration, in addition to the stoichiometric nutrient balance. Therefore, the complete consumption of the additional DIN supply is a possibility owing to its extremely low level in June.

In September, when the autumn bloom began, a rapid decrease in the mean salinity in the water column owing to high precipitation was also observed (Fig. 2b,c). This suggests that an additional supply of nitrogen derived

from rainfall and riverine discharges occurred in that month as well as in June. The DIN concentration in August (0.5–0.6 μM), immediately before the occurrence of the autumn bloom, was one of the lowest observed in the year (Fig. 3b). Hence, additional nitrogen inputs would have also impacted phytoplankton dynamics in September. Moreover, September was the month in which the vertical mixing of the water column began (Fig. 2a). In the Seto Inland Sea, the collapse of seasonal stratification followed by vertical mixing is usually observed in early autumn (Kobayashi et al. 2007). As was the case in the present study (Fig. 3b), this event in the Seto Inland Sea elevated the DIN concentration in the euphotic layer of the water column (Kobayashi et al. 2007). This generally occurs because the regenerative DIN stored in the aphotic layer is upwelled and supplied to the surface layer during the mixing period (Kobayashi et al. 2007). However, there is no aphotic layer in the water column in Shido Bay. Thus, the elevated DIN concentration during autumn in the bay (Fig. 3b) was possibly due to increased DIN concentrations in the outer area of the bay and its surroundings, caused by the initiation of vertical mixing outside the bay (i.e., there was an increase in the external DIN supply to the bay). Indeed, increased DIN concentrations from late summer to autumn have been observed in the Bisan Strait, the area adjacent to Shido Bay (Yamaguchi et al. 2015).

Taking all of the above into consideration, it is probable that an increased nitrogen supply in June and early autumn (i.e., September–October) triggered the phytoplankton blooms and the elevated phytoplankton production observed in these periods. The results of the present study emphasize the fact that DIN concentration is not always a good predictor of DIN supply, and that the latter is likely to be much more important than the former in elucidating the dynamics of phytoplankton production in Shido Bay.

The observed low phytoplankton production during winter (i.e., November–early January) was caused by low phytoplankton biomass with low Chl *a* specific productivity (Fig. 5). However, it is unclear why the latter two parameters remained low during winter despite high nutrient concentrations (Fig. 3). Our results indicate that mean Chl *a* specific productivity was positively correlated with temperature and light (see the "Phytoplankton biomass and production" section). Therefore, the lower temperature and $I_m$ in winter may have decreased Chl *a* specific productivity and prevented efficient nutrient utilization. However, if this is correct, the reason for the relative importance of temperature and $I_m$ compared to nutrients is unclear. As regards phytoplankton biomass, the low biomass in winter can be explained as follows: the observed low Chl *a* specific productivity reduced biomass accumulation, and the rapid increase in salinity after September (Fig. 2b) due to the enhancement of water exchange resulted in the promotion of biomass loss. To validate the above explanations, it is necessary to analyze seasonal changes in the water exchange rate between inner and outer Shido Bay in future studies.

Furthermore, in the present study, we did not analyze the representativeness of the estimated annual production and its variation. The annual mean phytoplankton biomass determined in this study ($17 \pm 15$ mg Chl *a* $m^{-2}$) is typical of that calculated for Shido Bay during the 2010s [16–27 mg Chl *a* $m^{-2}$ (Yamaguchi et al. 2017)], but the dependence of production on biomass may be variable. Therefore, further study is necessary to clarify the above points.

**Acknowledgements** We would like to express our appreciation to Koji Kishimoto, captain of the R/V Calanus III, for assistance with field observations. We also would like to thank Editage (www.editage.com) for the English language editing of an earlier version of the manuscript. This study was partly supported by the Coastal Ecosystem Complex Project of the Ministry of Education, Culture, Sports, Science and Technology, Japan.

## References

Adachi K, Nakayama A (2009) Environmental conditions as limiting factors in primary productivity in disposed coastal area. J JSCE Ser B 65:1131–1135 **(in Japanese with English abstract)**

Ara K, Yamaki K, Wada K, Fukuyama S, Okutsu T, Nagasaka S, Shiomoto A, Hiromi J (2011) Temporal variability in physicochemical properties, phytoplankton standing crop and primary production for 7 years (2002–2008) in the neritic area of Sagami Bay, Japan. J Oceanogr 67:87–111

Ara K, Fukushima S, Okutsu T, Nagasaka S, Shiomoto A (2019) Seasonal variability in phytoplankton carbon biomass and primary production, and their contribution to particulate carbon in the neritic area of Sagami Bay, Japan. Plankton Benthos Res 14:224–250

Cassis D, Pearce CM, Maldonado MT (2011) Effects of the environment and culture depth on growth and mortality in juvenile Pacific oysters in the Strait of Georgia, British Columbia. Aquacult Environ Interact 1:259–274

Cloern JE (1999) The relative importance of light and nutrient limitation of phytoplankton growth: a simple index of coastal ecosystem sensitivity to nutrient enrichment. Aquat Ecol 33:3–16

Cloern JE, Foster SQ, Kleckner AE (2014) Phytoplankton primary production in the world's estuarine-coastal ecosystems. Biogeosciences 11:2477–2501

Daneri G, Dellarossa V, Quiñones R, Jacob B, Montero P, Ulloa O (2000) Primary production and community respiration in the Humboldt Current system off Chile and associated oceanic areas. Mar Ecol Prog Ser 197:41–49

Dring MJ, Jewson DH (1982) What does $^{14}C$ uptake by phytoplankton really measure? A theoretical modelling approach. Proc R Soc Lond B 214:351–368

Emmery A, Allunno-Bruscia M, Bataillé MP, Kooijman SALM, Lefebvre S (2016) Dynamics of stable isotope ratios ($\delta^{13}C$ and $\delta^{15}N$) in different organs of *Crassostrea gigas* at two contrasted ecosystems: insights from growth and food sources. Vie Milieu 66:261–273

Endo T (1964) On primary production in Bingo-Nada of the Seto Inland Sea. I. Primary production and hydrographic condition. J Fac Fish Anim Husb Hiroshima Univ 5:503–518 **(in Japanese)**

Endo T (1970) On primary production in the Seto Inland Sea. J Fac Fish Anim Husb Hiroshima Univ 9:177–221 **(in Japanese)**

Eppley RW (1972) Temperature and phytoplankton growth in the sea. Fish Bull 70:1063–1085

e-Stat (2019) Annual statistics of fishery and aquaculture production, fiscal year 2018. https://www.e-stat.go.jp/stat-search/files/data?sinfid=000031824092&ext=xls. Accessed Nov 2019 (in Japanese)

Fisher TR, Peele ER, Ammerman JW, Harding LW Jr (1992) Nutrient limitation of phytoplankton in Chesapeake Bay. Mar Ecol Prog Ser 82:51–63

Foden J, Sivyer DB, Mills DK, Devlin MJ (2008) Spatial and temporal distribution of chromophoric dissolved organic matter (CDOM) fluorescence and its contribution to light attenuation in UK waterbodies. Estuar Coast Shelf Sci 79:707–717

Genkai-Kato M, Onishi M, Doi H, Nozaki K, Yoshino K, Miyasaka H, Omori K (2008) Photosynthetic property and primary production of phytoplankton in sublittoral sand bank area in the Seto Inland Sea. Ecol Res 23:1025–1032

Grundle DS, Timothy DA, Varela DE (2009) Variations of phytoplankton productivity and biomass over an annual cycle in Saanich Inlet, a British Columbia fjord. Cont Shelf Res 29:2257–2269

Hama T, Miyazaki T, Ogawa Y, Takahashi M, Otsuki A, Ichimura S (1983) Measurement of photosynthetic production of a marine phytoplankton population using a stable $^{13}C$ isotope. Mar Biol 73:31–36

Hashimoto S, Saino T (2004) Measurement and problem of primary production in the ocean. Oceanogr Jpn 13:357–370

Hirata Y, Akashige S (2004) The present situation and problems of oyster culture in Hiroshima Bay. Bull Fish Res Agen Suppl 1:5–12

Ho AYT, Xu J, Yin K, Jiang Y, Yuan X, He L, Anderson DM, Lee JHW, Harrison PJ (2010) Phytoplankton biomass and production in subtropical Hong Kong waters: influence of the Pearl River outflow. Estuaries Coasts 33:170–181

Holm-Hansen O, Lorenzen CJ, Holmes RW, Strickland JDH (1965) Fluorometric determination of chlorophyll. J Cons Perm Int Explor Mer 30:3–15

Inui M (2013) Encyclopedia of oyster farming in Japan. Suisan Shinko 544:1–120 **(in Japanese)**

Jeffrey SW, Humphrey GF (1975) New spectrophotometric equations for determining chlorophylls *a*, *b*, $c_1$ and $c_2$ in higher plants, algae and natural phytoplankton. Biochem Physiol Pflanzen 167:191–194

Joh H (1986) Studies on the mechanism of eutrophication and the effect of it on fisheries production in Osaka Bay. Bull Osaka Pref Fish Exp Stat 7:1–174 **(in Japanese)**

Justić D, Rabalais NN, Turner RE, Dortch Q (1995) Changes in nutrient structure of river-dominated coastal waters: stoichiometric nutrient balance and its consequences. Estuar Coast Shelf Sci 40:339–356

Kaeriyama H, Ichimi K, Tada K (2011) Seasonal and long-term changes in environmental physical conditions, nutrients and chlorophyll a concentration in Shido Bay, a coastal bay of the Seto Inland Sea, Japan. Umi to Sora 86:25–33 **(in Japanese with English abstract)**

Kobayashi S, Fujiwara T, Harashima A (2007) Seasonal and interannual variation of dissolved inorganic nitrogen in the Seto Inland Sea. Bull Coast Oceanogr 44:165–175 **(in Japanese with English abstract)**

Koga H (1990) Relationships between quantum and sunshine duration, global solar radiation, and growth of diatoms. Bull Saga Prefect Ariake Fish Res Dev Cent 12:67–74 **(in Japanese with English abstract)**

Lohrenz SE (1993) Estimation of primary production by the simulated in situ method. ICES Mar Sci Symp 197:159–171

Marañón E, Behrenfeld MJ, González N, Mouriño B, Zubkov MV (2003) High variability of primary production in oligotrophic waters of the Atlantic Ocean: uncoupling from phytoplankton biomass and size structure. Mar Ecol Prog Ser 257:1–11

Marra J (2004) The compensation irradiance for phytoplankton in nature. Geophys Res Lett 31:L06305

Miyagawa M, Fujiwara M (2011) Research on the nutrient concentrations around the laver culture farm in Shido Bay. Bull Kagawa Pref Fish Exp Stn 12:9–12 **(in Japanese with English abstract)**

Montecino V, Quiroz D (2000) Specific primary production and phytoplankton cell size structure in an upwelling area off the coast of Chile. Aquat Sci 62:364–380

Nakai S, Soga Y, Sekino S, Umehara A, Okuda T, Ohno M, Nishijima W, Asaoka S (2018) Historical changes in primary production in the Seto Inland Sea, Japan, after implementing regulations to control the pollutant loads. Water Policy 20:855–870

Ohara S, Yano R, Hagiwara E, Yoneyama H, Koike K (2020) Environmental and seasonal dynamics of altering the primary productivity in Bingo-Nada (Bingo Sound) of the Seto Inland Sea. Plankton Benthos Res 15:78–96

Örnólfsdóttir EB, Lumsden SE, Pinckney JL (2004) Phytoplankton community growth-rate response to nutrient pulses in a shallow turbid estuary, Galveston Bay, Texas. J Plankton Res 26:325–339

Parsons TR, Takahashi M, Hargrave B (1984) Biological oceanographic processes, 3rd edn. Pergamon, Oxford

Riley GA (1957) Phytoplankton of the north central Sargasso Sea, 1950–52. Limnol Oceanogr 2:252–270

Rysgaard S, Nielsen TG, Hansen BW (1999) Seasonal variation in nutrients, pelagic primary production and grazing in a high-Arctic coastal marine ecosystem, Young Sound, Northeast Greenland. Mar Ecol Prog Ser 179:13–25

Shiomoto A (2011) Phytoplankton biomass and production in the coastal area of the Shiretoko Peninsula during late spring to early autumn: comparison between the Okhotsk Sea and the Nemuro Straight. Bull Coast Oceanogr 49:37–48 **(in Japanese with English abstract)**

Srithongouthai S, Tada K (2017) Impacts of organic waste from a yellowtail cage farm on surface sediment and bottom water in Shido Bay (the Seto Inland Sea, Japan). Aquaculture 471:140–145

Srithongouthai S, Sonoyama Y, Tada K, Montani S (2003) The influence of environmental variability on silicate exchange rates between sediment and water in a shallow-water coastal ecosystem, the Seto Inland Sea, Japan. Mar Pollut Bull 47:10–17

Strickland JDH, Parsons TR (1972) A practical handbook of seawater analysis. Fisheries Research Board of Canada, Ottawa

Suenaga Y, Tomizawa N, Masuda K, Montani S, Tada K (2002) Modeling of dissolved oxygen of aquaculture grounds in a semi-enclosed bay. Fish Sci 68:546–549 **(Sup. I)**

Tada K (1998) Nitrogen and phosphate concentrations in rainwater and nutrient loading due to rainfall on coastal environment. Umi Sora 73:125–130 **(in Japanese with English abstract)**

Tada K, Morishita M (1997) The changes of environmental chemical conditions and biomass on lower trophic levels in a coastal bay. Tech Bull Fac Agric Kagawa Univ 49:35–47 **(in Japanese with English abstract)**

Tada K, Monaka K, Morishita M, Hashimoto T (1998) Standing stocks and production rates of phytoplankton and abundance of bacteria in the Seto Inland Sea, Japan. J Oceanogr 54:285–295

Tada K, Morishita M, Hamada K, Montani S, Yamada M (2001) Standing stock and production rate of phytoplankton and a red tide outbreak in a heavily eutrophic embayment, Dokai Bay, Japan. Mar Pollut Bull 42:1177–1186

Tanaka K, Kodama M, Sawada T, Tsuzuki M, Yamamoto Y, Yanagisawa T (2009) Flood event loadings of nitrogen and phosphorus from the Yahagi River to Chita Bay, Japan. JARQ Jpn Agr Res Quart 43:55–61

Timothy DA, Soon MYS (2001) Primary production and deep-water oxygen content of two British Columbian fjords. Mar Chem 73:37–51

Uye S, Kuwata H, Endo T (1987) Standing stocks and production rates of phytoplankton and planktonic copepods in the Inland Sea of Japan. J Oceanogr Soc Japan 42:421–434

Yamaguchi M, Anraku M (1984) Primary productivity in Suo-Nada, western Seto Inland Sea. Bull Nansei Reg Fish Res Lab 17:135–149 **(in Japanese with English abstract)**

Yamaguchi M, Imai I (1996) Size fractionated phytoplankton biomass and primary productivity in Osaka Bay, eastern Seto Inland Sea, Japan. Bull Nansei Natl Fish Res Inst 29:59–73

Yamaguchi M, Imai I, Matsuo Y (1995) Seasonal changes in biomass and photosynthetic rate of phytoplankton in Hiroshima Bay. Bull Nansei Natl Fish Res Inst 28:63–72 **(in Japanese with English abstract)**

Yamaguchi H, Hirade N, Higashizono K, Tada K, Kishimoto K, Oyama K, Ichimi K (2015) Light and nutrient limitation on phytoplankton production in the strait of an enclosed coastal sea (Bisan Strait, eastern Seto Inland Sea, Japan). J Sea Res 103:75–83

Yamaguchi H, Tamura T, Ichimi K, Tada K (2017) Effects of phytoplankton on light attenuation in "shallow coastal photic systems": a case study in the Shido Bay, eastern Seto Inland Sea, Japan. Bull Plankton Soc Japan 64:29–34 **(in Japanese with English abstract)**

Yamashita A, Iseki K, Tarutani K, Koizumi Y (2011) Seasonal variation of primary productivity in Shitaba Bay of Uwa Sea, Japan. Bull Jpn Soc Fish Oceanogr 75:9–18 **(in Japanese with English abstract)**